Steel and Composite Structures, *Vol. 18, No. 5 (2015) 1259-1277*
DOI: http://dx.doi.org/10.12989/scs.2015.18.5.1259

Behavior and design of perforated steel storage rack columns under axial compression

Bassel El Kadi [*1] and G. Kiymaz [2]

[1] *Department of Civil Engineering, Faculty of Engineering, Fatih University, Buyukcekmece Campus, Istanbul, Turkey*
[2] *Department of Civil Engineering, Faculty of Engineering, Antalya International University, Dosemealti, Antalya, Turkey*

(*Received August 08, 2014, Revised November 10, 2014, Accepted November 17, 2014*)

Abstract. The present study is focused on the behavior and design of perforated steel storage rack columns under axial compression. These columns may exhibit different types of behavior and levels of strength owing to their peculiar features including their complex cross-section forms and perforations along the member. In the present codes of practice, the design of these columns is carried out using analytical formulas which are supported by experimental tests described in the relevant code document. Recently proposed analytical approaches are used to estimate the load carrying capacity of axially compressed steel storage rack columns. Experimental and numerical studies were carried out to verify the proposed approaches. The experimental study includes compression tests done on members of different lengths, but of the same cross-section. A comparison between the analytical and the experimental results is presented to identify the accuracy of the recently proposed analytical approaches. The proposed approach includes modifications in the Direct Strength Method to include the effects of perforations (the so-called reduced thickness approach). CUFSM and CUTWP software programs are used to calculate the elastic buckling parameters of the studied members. Results from experimental and analytical studies compared very well. This indicates the validity of the recently proposed approaches for predicting the ultimate strength of steel storage rack columns.

Keywords: steel storage rack columns; reduced thickness method; elastic buckling; thin-walled columns; finite element analysis; finite strip method

1. Introduction

Steel storage rack columns face difficulties for their design as different manufacturers apply different complex forms of cross-sections with various forms of perforations existing along their lengths. As a result, cold-formed steel storage rack columns cannot be designed based on a unified design method. The non-linear finite element analysis is considered to be the best alternative to experimental testing, but still it cannot be considered as a practical way for designing. Hence research studies were carried out to determine the possibility of finding an analytical procedure for

*Corresponding author, Ph.D. Student, E-mail: bassel_elkadi@hotmail.com

http://www.techno-press.org/?journal=scs&subpage=8 ISSN: 1229-9367 (Print), 1598-6233 (Online)

checking the strength and stability of rack columns. In the North American Specification there are two basic design methods for cold-formed steel members. The first one is Effective Width Method, which was originally introduced by Von Karman *et al*. (1932) and it is the traditional design method available world-wide for formal use in design. The Direct Strength Method (DSM), which is also known as the Appendix 1 method, was included as an alternative design method in the 2001 edition of the North American Specification. Comprehensive information on the background and use of DSM is given in a design guide by Schafer (2006a). In a review paper by Schafer (2008) it is noted that the reliability of the Direct Strength Method is as good as the Effective Width Method.

One of the above mentioned design methods could be selected to design a cold formed steel storage rack column. However to consider the possible effect of perforations present one should refer to the available codified rules for the design of cold formed steel rack columns. These rules include additional recommendations for handling the effect of perforations. Due to the fact that manufacturers of rack structural members employ various forms and dimensions of perforations, the effect of perforations on column strength is taken into account by testing. Axial compression tests are carried out on stub columns to find out the level of strength reduction due to perforations as well as local buckling of cross-section.

In an effort to eliminate the need for such tests, recently, an investigation was carried out by Casafont *et al*. (2013) to explore the possibility of developing an analytical procedure for checking the strength and stability of rack columns. In this study the aim was to adapt the existing procedures for design of non-perforated column members to be applied for the strength prediction of perforated rack columns. An attempt to predict the load carrying capacity of perforated rack columns by the Direct Strength Method (DSM) was presented. The investigation focused on two different issues. The first was to predict the elastic buckling loads of members with multiple perforations. For this purpose, a procedure for the calculation of elastic buckling loads of perforated members by the finite strip method was presented. The calculations were carried out by using the finite strip software CUFSM developed by Schaffer (1997). The concept of reduced thickness of the perforated strip is adopted to include the effect of holes, by using finite element analysis to calibrate different formulas for the calculation of reduced thickness values to be used in CUFSM models. The second issue that the investigation has focused on was to evaluate the accuracy of the current Direct Strength Method strength curves when they are applied to rack columns. Satisfactory results were obtained when they were compared with experimental values.

The aim of the present study is to confirm, through providing additional experimental data, the validity of the aforementioned analytical approach proposed and adopted by Casafont *et al*. (2013). For this purpose, an experimental study was carried out on a number of cold formed steel storage rack columns with selected rack cross-section geometry and with varying column lengths. As per the adopted approach, the Direct Strength Method incorporating the so-called reduced thickness method was used for the prediction of the test specimen strengths. For the prediction of elastic local, distortional and global buckling loads CUFSM and CUTWP software programs were used. Comparisons made between the test results and the proposed approach in terms of nominal ultimate strength values were found to be supportive of the validity of the newly proposed approach.

2. Experimental study

2.1 Description of the test specimens

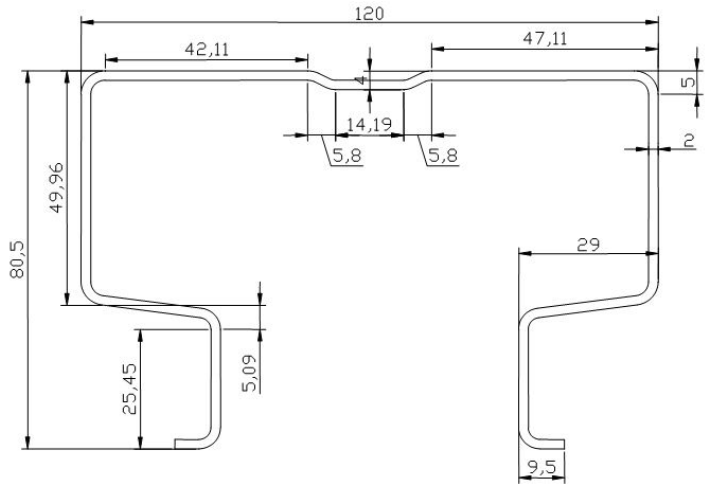

Fig. 1 Cross-section of the test specimen (dimensions in mm)

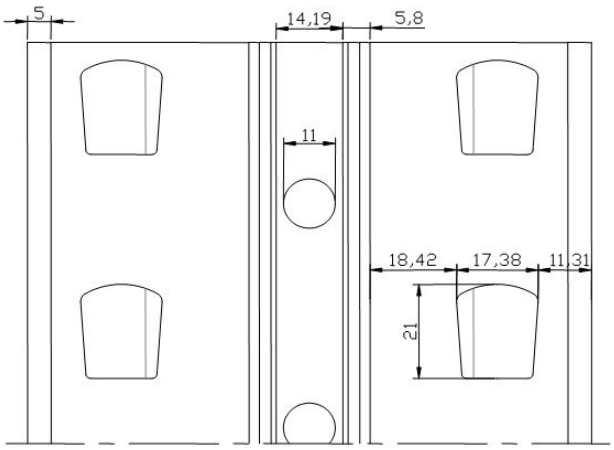

Fig. 2 Web perforations of the test specimen (dimensions in mm)

Experimental tests are carried out to estimate the load carrying capacity of axially loaded compressed steel storage rack columns. Members of the same cross-section but of six different lengths (500, 650, 800, 950, 1,100, and 1,250 mm) are tested. The dimensions of the tested cross-section are shown in Figs. 1-3.

2.2 Test arrangement

The tests are carried out in a compression test machine of 1,000 kN capacity. At both ends of the specimen, a 30 mm thick load distribution steel plate is fixed as shown in Fig. 4.The load was applied to the specimen by means of a steel piston that has a spherical end of 30 mm diameter acting on a conic seat, drilled in the center of the outer face of the load distribution steel plate. These two spherical ends specify accurately the line of application of the load. The tests are carried

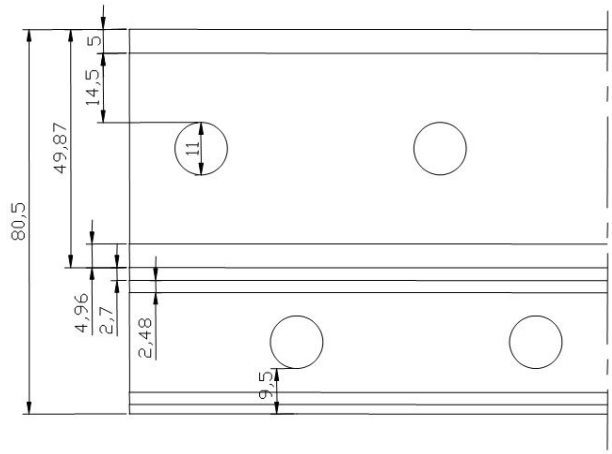

Fig. 3 Flange perforations of the test specimen (dimensions in mm)

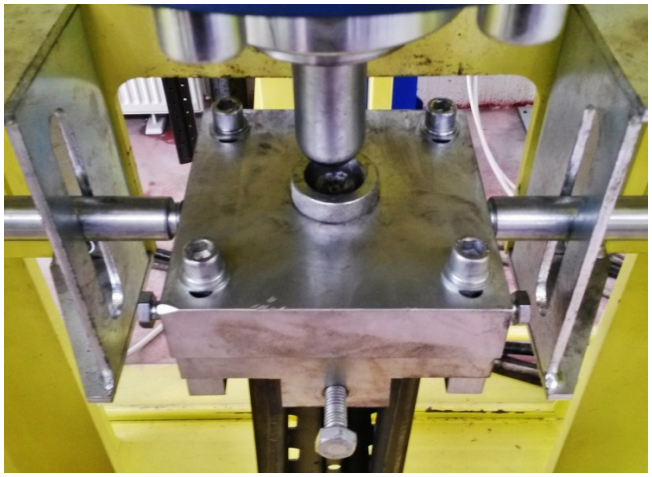

Fig. 4 Boundary condition of the test

out by a gradual increasing of the load, until the column reaches the ultimate failure mode. Tests are load controlled at a loading rate of 200 N/s.

2.3 Test boundary conditions

The test specimen is torsional restrained using the two bolts which are connected to the load distribution steel plate. The load is applied frictionless through the piston to the conic seat which is on the outer surface of the load distribution steel plate, as shown in Fig. 4. The column ends are bolted to the end grips, which makes it easier to replace the specimen quickly once the test is finished, compared to welding the specimen to end plates. Clamping the column ends to the end grips using bolts, leads to an end condition very similar to a fixed end according to local and distortional buckling modes.

2.4 Determination of the center of gravity

It is not easy to use analytical calculations to determine an accurate value for the center of gravity of a steel storage rack column, due to the existence of the perforations along its length. Therefore, in this study the effective center of gravity of the cross-section is determined by an experimental method as described in EN15512 (2009). A series of seven tests are done, in each test the load application point was changed, along the symmetry plane of the cross-section. The effective center of gravity of the section is determined by investigating the position that gives the maximum ultimate failure load (Roure *et al*. 2011). The failure loads are plotted against the position of the load line. The maximum of this curve is the experimental failure load of the section which corresponds to the effective center of gravity of the section, as shown in Fig. 5. The load-displacement graph is plotted for each of the seven columns used for determining the effective center of gravity of the tested cross-section. The curves for the different columns were drawn together in Fig. 6.

In Fig. 6 it was observed that all the seven curves are bounded by the curve for C360-g-01 and the curve for C360-g-05. The curve for C360-g-01 is the upper bound curve and it is for the case where the load is applied at the effective center of gravity, at which we get the maximum ultimate load. The curve for C360-g-05 is the lower bound curve and it is for the case where the load is applied at the furthest load application point from the effective center of gravity, at which we get the lowest ultimate load. The upper bound C360-g-01 curve exhibits the highest initial stiffness behavior, where the lower bound C360-g-05 curve exhibits the lowest initial stiffness behavior.

It was observed from Fig. 5 that the center of gravity of the cross-section in which the maximum load is obtained is at $x = 37$ mm. When the load is not applied on the effective center of gravity, two different buckling cases occur because of the eccentricity.

First case, for $x < 37$ mm, eccentricity of the load produces a moment, which will apply a compressive force on the web of the cross-section as shown in Fig. 7(a). As a result of that, the buckling takes place at the web as shown in Fig. 7(b).

Second case, for $x > 37$ mm, eccentricity of the load produces a moment, which will apply a compressive force on the flanges of the cross-section as shown in Fig. 8(a). As a result of that the

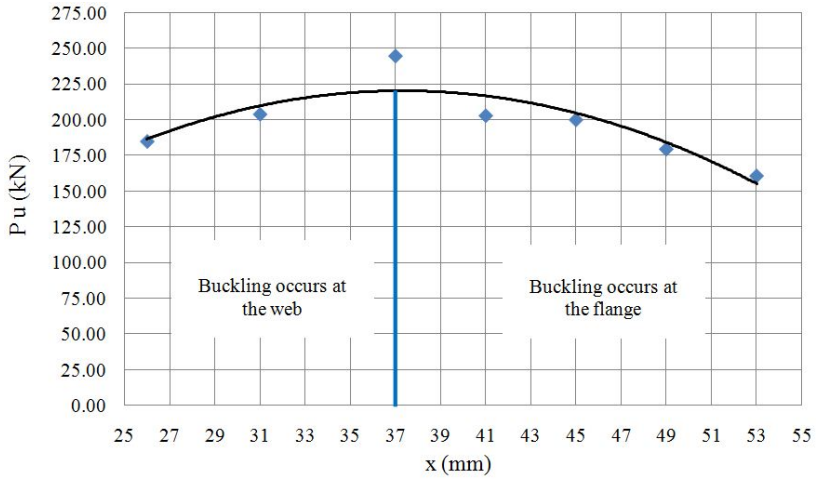

Fig. 5 Experimental results to find the effective center of gravity of the section

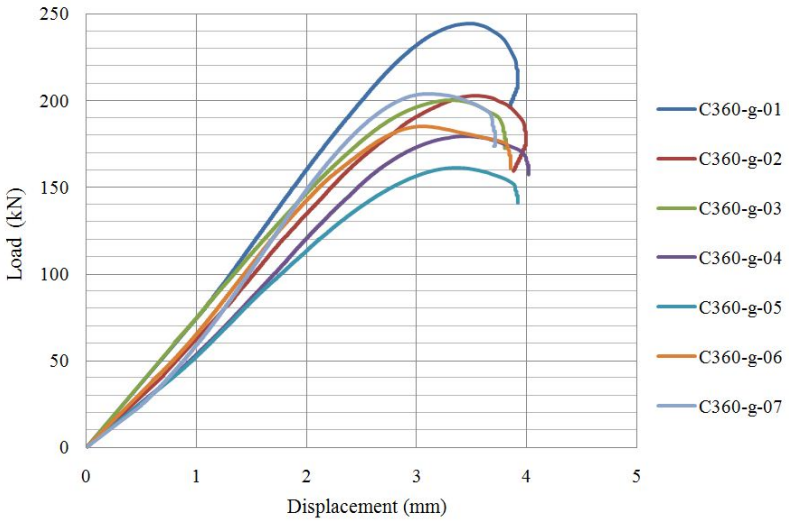

Fig. 6 Load-displacement curves for the columns used to determine the effective center of gravity of the tested cross-section

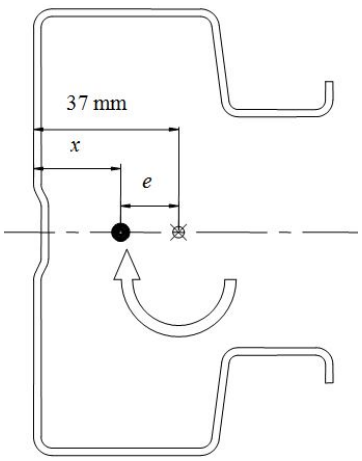

(a) Moment occurs and compresses the web

(b) Buckling occurs at the web

Fig. 7 Moment occurs and compresses the web leading to its buckling

buckling takes place at the flanges as show in Fig. 8(b).

2.5 Stub column test

The length of the stub column is calculated as follows:

- The length shall be greater than three time the greatest flat width of the section

$$L \geq 3W = 3 \times 120 = 360 \text{ mm} \quad (1)$$

where W is the greatest flat width of the section.

- The length shall include at least five pitches of the perforations

$$L \geq 5P = 5 \times 50 = 250 \text{ mm} \tag{2}$$

where P is the pitch of perforations.

The chosen specimen length is 360 mm, and the axial compression load is applied at the effective center of gravity.

Table 1 shows the ultimate loads of the stub column tests and the resulting Q factors, while the Q which is the capacity reduction factor is determined with the following equation

$$Q = \frac{P_{u,s}}{F_y A_{net\,\min}} \tag{3}$$

where

$P_{u,s}$ = the ultimate compressive strength from stub column tests

F_y = the yield stress of the column material

$A_{net\min}$ = the minimum cross sectional area obtained by passing a plane through the column normal to the axis of the column

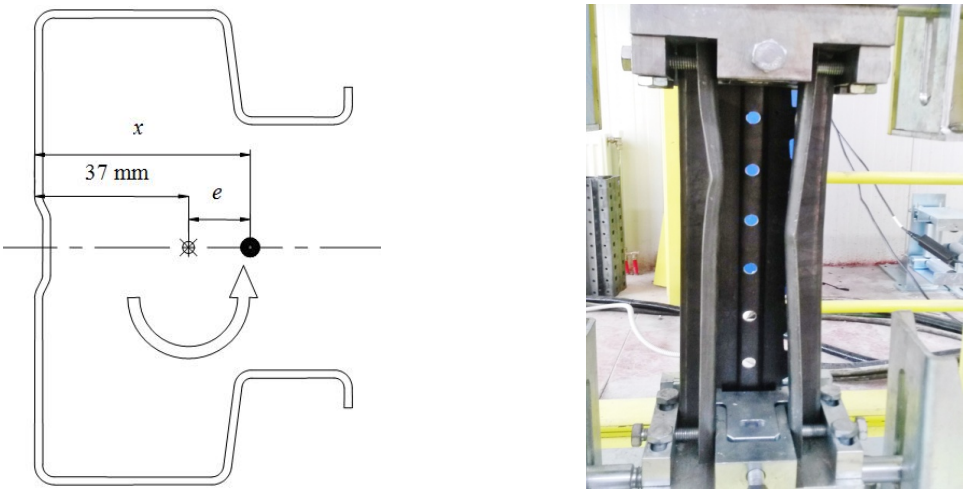

(a) Moment occurs and compresses the flanges (b) Buckling occurs at the flanges

Fig. 8 Moment occurs and compresses the flanges leading to its buckling

Table 1 Stub column test results

Column	*P* (kN)	*tf*1 (mm)	*tw*1 (mm)	*tw*2 (mm)	*tf*2 (mm)	*t* (mm)	*t av* (mm)	*Pu* (kN)	*A net min* (mm²)	*Q*
C360-01	255.51	2.24	2.28	2.28	2.23	2.26				
C360-02	244.50	2.22	2.20	2.20	2.23	2.21	2.25	249.32	662.63	1
C360-03	247.96	2.23	2.32	2.34	2.25	2.29				

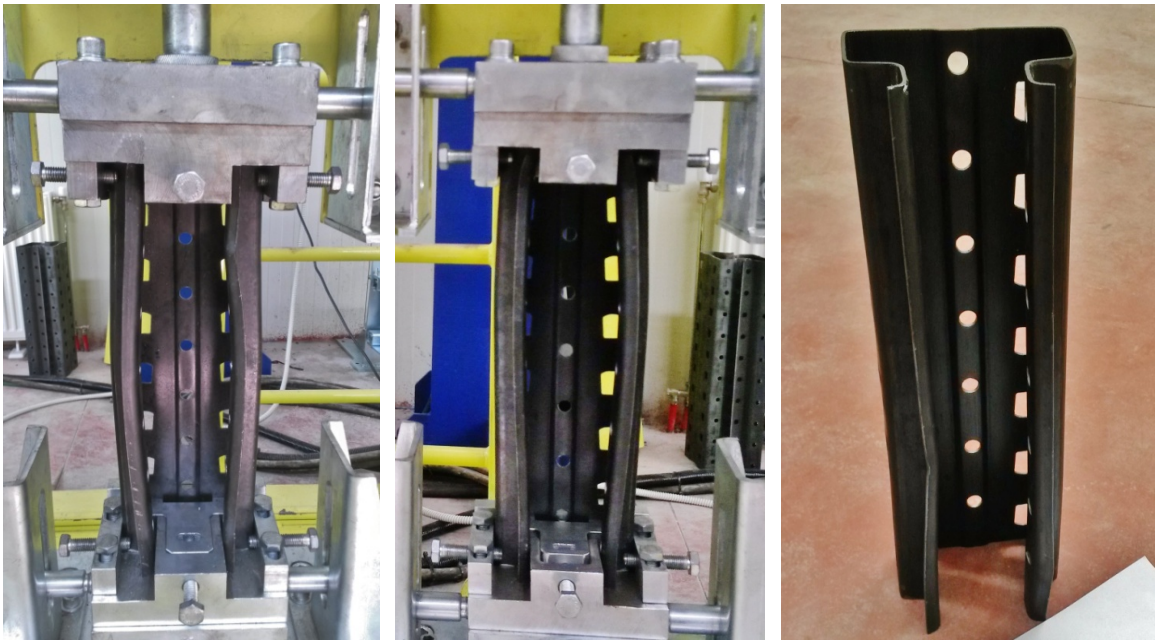

(a) (b) (c)

Fig. 9 Failure mode of stub columns

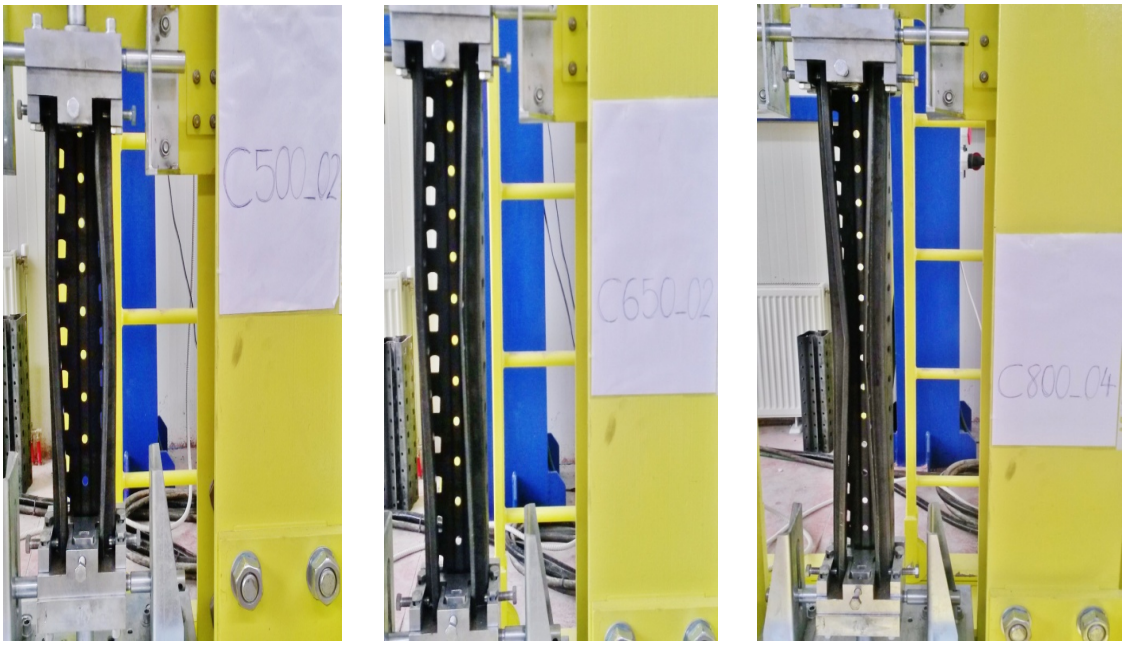

(a) 500 mm (b) 650 mm (c) 800 mm

Fig. 10 Failure mode of columns of different lengths

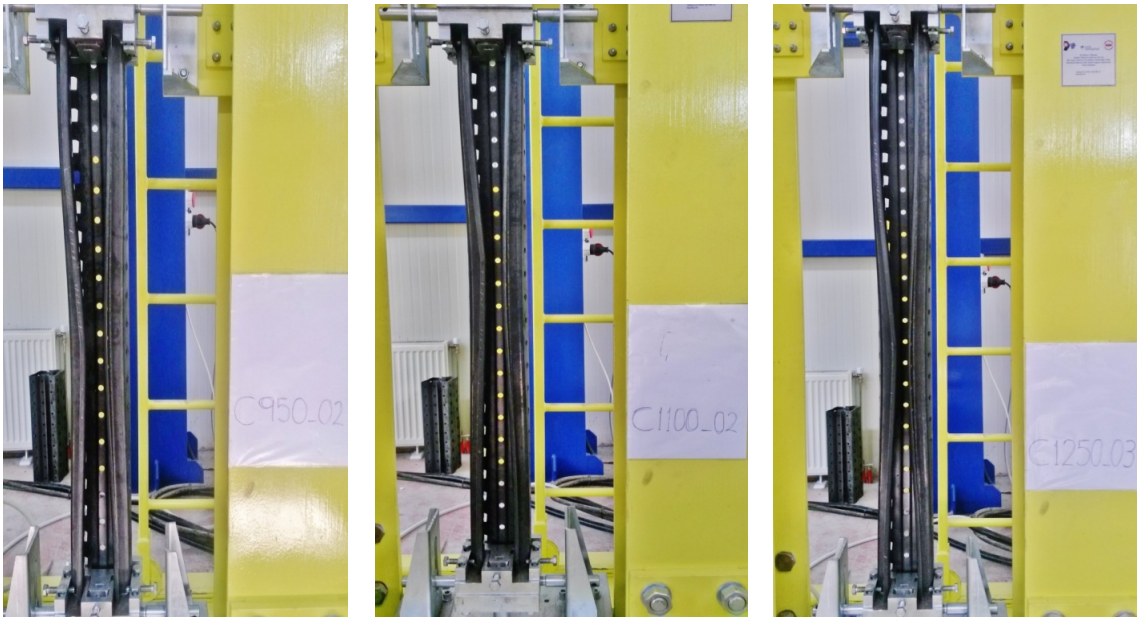

(a) 950 mm (b) 1100 mm (c) 1250 mm

Fig. 11 Failure mode of columns of different lengths

The stub column test results showed that the chosen cross-sections were not susceptible to local buckling. All the stub columns failed in distortional mode. An average value of yield stress close to 355 Mpa (nominal value for S355) was found and it was decided to adapt the nominal value of yield stress. In Table 1, using Fy = 355 Mpa results in a value of Q factor equal to unity.

2.6 Tests on rack columns of different lengths

Tests are carried out to determine the ultimate failure load of the steel storage rack columns with six different lengths (500, 650, 800, 950, 1,100, and 1,250 mm). The compressive load is applied on the effective center of gravity which is determined in Section 2.4. Figs 10-11 show an example for the elastic failure modes observed from some of the test specimens.

2.7 Test results

Fig. 12 shows the relationship between load and displacement for the test specimens, to the different column lengths. As the column length increases, the stiffness and the ultimate failure load of the column decrease. Displacements levels correspond to the maximum loads are close. It is observed that distortional buckling was the dominating buckling mode for all of the tests. For columns of length 1,250 and 1,100 mm, small effect of flexural buckling was noticed. The results obtained from the experimental tests are shown in Table 2.

The results of the tests for columns C650-01, C800-03, and C1250-02 were neglected while calculating the average ultimate failure load, due to the big difference in their ultimate load compared to the results of the other columns of the same length. Four readings were taken in order

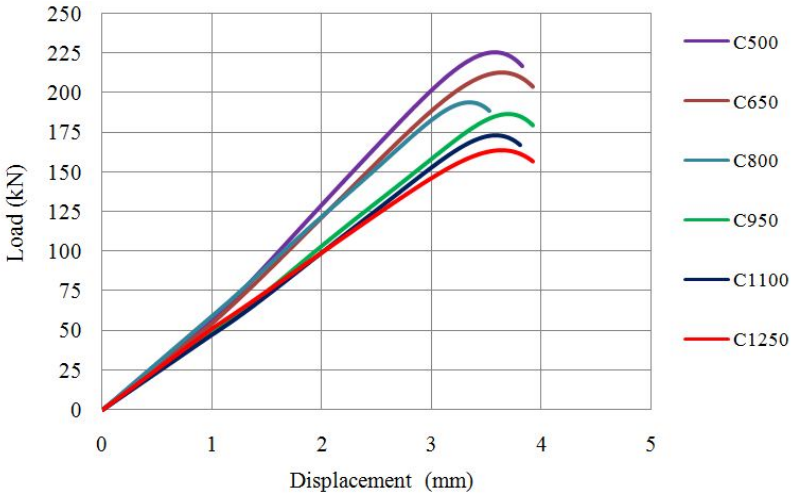

Fig. 12 Relationship between load and displacement for the test specimens of different length

Table 2 Experimental results

	Column	*P* (kN)	*tf*1 (mm)	*tw*1 (mm)	*tw*2 (mm)	*tf*2 (mm)	*t* (mm)	*t av* (mm)	*Put* (kN)
1	C500-01	226.91	2.15	2.09	2.11	2.00	2.09	2.13	224.18
	C500-02	225.54	2.00	2.05	2.02	2.09	2.04		
	C500-03	220.10	2.20	2.25	2.25	2.29	2.25		
2	C650-01	194.67	2.09	2.11	2.10	2.09	2.10	2.13	208.86
	C650-02	203.53	2.14	2.12	2.12	2.14	2.13		
	C650-03	211.36	2.11	2.11	2.13	2.11	2.12		
	C650-04	211.69	2.14	2.16	2.12	2.16	2.15		
3	C800-01	199.10	2.13	2.14	2.12	2.13	2.13	2.13	195.56
	C800-02	195.77	2.16	2.15	2.16	2.13	2.15		
	C800-03	181.46	2.15	2.14	2.16	2.14	2.15		
	C800-04	191.80	2.13	2.10	2.10	2.09	2.11		
4	C950-01	197.41	2.16	2.15	2.16	2.14	2.15	2.14	190.58
	C950-02	188.85	2.14	2.16	2.14	2.14	2.15		
	C950-03	185.48	2.11	2.12	2.13	2.12	2.12		
5	C1100-01	172.18	2.11	2.11	2.11	2.11	2.11	2.11	172.30
	C1100-02	171.08	2.12	2.11	2.11	2.11	2.11		
	C1100-03	173.63	2.11	2.08	2.10	2.10	2.10		
6	C1250-01	172.67	2.12	2.12	2.11	2.12	2.12	2.13	170.61
	C1250-02	179.47	2.01	2.01	2.05	2.20	2.02		
	C1250-03	163.45	2.15	2.12	2.12	2.14	2.13		
	C1250-04	175.71	2.13	2.14	2.14	2.17	2.14		

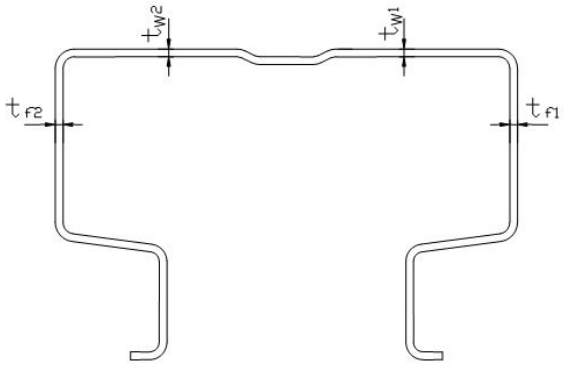

Fig. 13 Measured thicknesses for the test specimen

to determine the average thickness of the tested cross-sections, according to what is shown in Fig. 13.

3. Analytical study

Analytical study is carried out according to the aforementioned analytical procedure recently proposed by Casafont *et al*. (2013). In this study, using the reduced thickness approach, results from the finite strip analysis software CUFSM and CUTWP programs, and results from stub column tests will be used as inputs for the equations.

3.1 Analytical procedures

It was stated that, it is better to model the distortional buckling by using the finite strip method analysis using CUFSM3 and CUFSM4 programs, by applying the reduced thickness approach while modelling the effect of perforations in the strips containing perforations (Casafont *et al*. 2013). However, for determining the overall flexural or torsional-flexural buckling stress, CUTWP program is the most suitable program. It was mentioned that the best way to determine the local buckling effect is to calculate the capacity reduction factor Q, using the results obtained from the stub column test, where Q is calculated as mentioned in Eq. (3).

The ultimate strength is calculated according to different alternatives of modified versions of the Direct Strength Method. These alternatives are described below:

- Step 1: The elastic global buckling load P_{cre} is determined by CUTWP program using the reduced thickness method.
- Step 2: The distortional buckling load P_{crd} is determined by CUFSM program using the reduced thickness method.
- Step 3: The local-global buckling strength P_{nel} is determined as

$$P_{nel} = \left(1 - (1 - Q)\left(\frac{P_{ne}}{P_y}\right)^{Q}\right) P_{ne} \tag{4}$$

where

Q = The capacity reduction factor calculated according to Eq. (3).

P_y = $A_{net\min}F_y$ = The yield strength of the column.

P_{ne} = The nominal axial strength for the flexural, torsional, or flexural-torsional buckling, which is being calculated according to the following equations:

For $\lambda_c \leq 1.5$

$$P_{ne} = \left(0.658^{\lambda_c{}^2}\right)P_y \tag{5}$$

For $\lambda_c > 1.5$

$$P_{ne} = \left(\frac{0.877}{\lambda_c{}^2}\right)P_y \tag{6}$$

where

$$\lambda_d = \sqrt{\frac{P_{ne}}{P_{crd}}} \tag{7}$$

- Step 4: Different alternatives are used for determining the nominal axial strength for distortional buckling P_{nd}.

3.1.1 Alternative 1

The nominal axial strength, P_{nd}, for distortional buckling is calculated according to the following equations:

For $\lambda_d \leq 0.561$

$$P_{nd} = P_{ne} \tag{8}$$

For $\lambda_d > 0.561$

$$P_{nd} = \left[1 - 0.25\left(\frac{P_{crd}}{P_{ne}}\right)^{0.6}\right]\left(\frac{P_{crd}}{P_{ne}}\right)^{0.6} P_{ne} \tag{9}$$

where

$$\lambda_d = \sqrt{\frac{P_{ne}}{P_{crd}}} \tag{10}$$

and P_{ne} = value as given in Eqs. (5)-(6).

P_{crd} = the distortional buckling load determined by the CUFSM program

The column strength is the lower of P_{nel} determined from Step 3 and P_{nd}.

3.1.2 Alternative 2

The nominal axial strength, P_{nd}, for distortional buckling is calculated according to the following equations:

For $\lambda_d \leq 0.561$

$$P_{nd} = P_{nel} \tag{11}$$

For $\lambda_d > 0.561$

$$P_{nd} = \left[1 - 0.25\left(\frac{P_{crd}}{P_{nel}}\right)^{0.6}\right]\left(\frac{P_{crd}}{P_{nel}}\right)^{0.6} P_{nel} \tag{12}$$

where

$$\lambda_d = \sqrt{\frac{P_{nel}}{P_{crd}}} \tag{13}$$

and P_{nel} = value as given in Eq. (4).
P_{crd} = the distortional buckling load determined by the CUFSM program
The column strength is P_{nd} determined here.

3.1.3 Alternative 3

The nominal axial strength, P_{nd}, for distortional buckling is calculated according to the following equations:

For $\lambda_d \leq 0.561$

$$P_{nd} = P_y \tag{14}$$

For $\lambda_d > 0.561$

$$P_{nd} = \left[1 - 0.25\left(\frac{P_{crd}}{P_y}\right)^{0.6}\right]\left(\frac{P_{crd}}{P_y}\right)^{0.6} P_y \tag{15}$$

where

$$\lambda_d = \sqrt{\frac{P_y}{P_{crd}}} \tag{16}$$

and P_y = the yield strength of the column, calculated according to Step 3
P_{crd} = the distortional buckling load determined by the CUFSM program
The column strength is the lower of P_{nel} determined from Step 3 and P_{nd}.

3.1.4 Alternative 4

It is the current RMI specification without calculating the distortional buckling strength explicitly. The calculations will stop at Step 3 and the column strength is equal to P_{nel}.

$$P_{nel} = \left(1 - (1 - Q)\left(\frac{P_{ne}}{P_y}\right)^{Q}\right) P_{ne} \tag{17}$$

3.2 Analytical results

The reduced thickness approach that was developed by Casafont *et al*. (2013) is being applied

to the studied cross-section. The reduced thicknesses that are used to indicate the rectangular and circular perforations in CUTWP and CUFSM programs are shown in Table 3. Fig. 14 shows the location of the strips at which the calculated reduced thicknesses are applied.

The following tables show the results obtained from the analytical studies, for all the different lengths of the tested column specimens. The results obtained from CUFSM and CUTWP programs,

Table 3 Reduced thickness values calculated for the perforated strips

Buckling mode	Reduced thickness equations	t_{rr} (rectangular perforations)	t_{rc} (circular perforations)
Local buckling	$t_{rL} = 0.61t\frac{L_{np}B_{np}}{L\,H} + 0.18t\frac{B_p}{L_p} + 0.11$	1.44 mm	1.22 mm
Distortional buckling	$t_{rD} = 0.9t\left(\frac{L_{np}}{L}\right)^{\frac{1}{3}}$	1.50 mm	1.66 mm
Global buckling	$t_{rG} = 0.7t\left(\frac{L_{np}}{L}\right)$	0.81 mm	1.09 mm

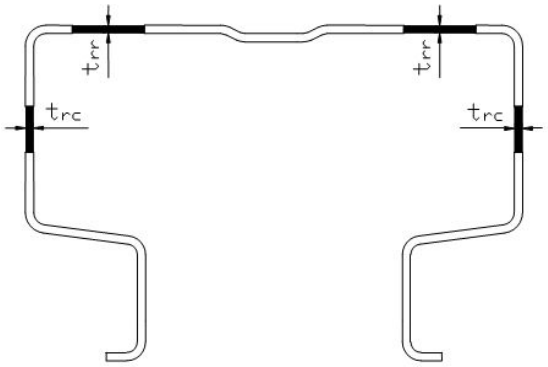

Fig. 14 Strips at which the calculated reduced thickness values are applied

Table 4 Results obtained from CUFSM and CUTWP programs

		Results from CUFSM					Results from CUTWP		
Length (mm)	*Pyl* (kN)	*Pcrl*/*Pyl*	*Pcrl* (kN)	*Pyd* (kN)	*Pcrd*/*Pyd*	*Pcrd* (kN)	*Pye* (kN)	*Pcre*/*Pye*	*Pcre* (kN)
500	236.40	3.26	770.39	240.57	3.58	861.42	227.63	10.34	2354.25
650	236.40	3.26	770.39	240.57	2.54	612.06	227.63	6.12	1394.95
800	236.40	3.26	770.39	240.57	1.89	454.44	227.63	4.05	922.46
950	236.40	3.26	770.39	240.57	1.54	369.64	227.63	2.87	655.50
1100	236.40	3.26	770.39	240.57	1.36	326.62	227.63	2.15	490.10
1250	236.40	3.26	770.39	240.57	1.28	309.04	227.63	1.67	380.58

Table 5 The nominal axial strength according to the different alternatives

Length (mm)	*Fy* (Mpa)	*Pn* (kN) *Alt 1*	*Pn* (kN) *Alt 2*	*Pn* (kN) *Alt 3*	*Pn* (kN) *Alt 4*
500	355	225.26	225.26	225.26	225.26
650	355	217.67	217.67	218.87	218.87
800	355	202.00	202.00	211.11	211.11
950	355	186.21	186.21	202.16	202.16
1100	355	173.44	173.44	192.13	192.13
1250	355	163.58	163.58	181.35	181.35

which are used as inputs for the calculation of the nominal column strength using the alternatives mentioned in Section 3.1 are shown in Table 4. Table 5 shows the values of the nominal column strength determined according to the different alternatives.

4. Comparison between the experimental and analytical results

Calculations were carried out to determine the nominal column strength by using DSM without considering the effect of perforations, which is the current method in the design code. The obtained results were compared to the experimental results in Table 6. The nominal column strengths determined from the different alternatives mentioned in Section 3.1, are compared to the average ultimate failure load obtained from the test results, which were determined as shown in Table 7. The ratio between the calculated nominal column strength and the ultimate load failure was calculated to indicate the accuracy of the different alternatives as shown in Table 7.

Alternative 1 and Alternative 2 are equal, because the calculated capacity reduction factor Q is equal to 1, which neglect the effect of local buckling that already did not occur in the experimental tests. Alternative 3 and Alternative 4 are equal for the tested cross-section. Graphs were plotted as shown in Figs. 15-16, to explain the difference of the results accuracy of the alternatives and the results obtained from the non-perforated model, compared to the different experimental results obtained from the tests and the average ultimate failure load.

Table 6 Comparison between experimental results and analytical results for the section without considering the effect of perforations

Length (mm)	*Fy* (Mpa)	*Pu* (kN) *Test1*	*Pu* (kN) *Test2*	*Pu* (kN) *Test3*	*Pu* (kN) *Test4*	*Put* (kN)	*Pn non per* (kN)	$\frac{Pn\ non\ per}{Put}$
500	355	226.91	225.54	220.10		224.18	240.11	1.0711
650	355	194.67	203.53	211.36	211.69	208.86	233.92	1.1200
800	355	199.10	195.77	181.46	191.80	195.56	226.38	1.1576
950	355	197.41	188.85	185.48		190.58	217.63	1.1419
1100	355	172.18	171.08	173.63		172.30	207.85	1.2063
1250	355	172.67	179.47	163.45	175.71	170.61	197.25	1.1561

Table 7 Comparison between the experimental and analytical results

Length (mm)	*Fy* (Mpa)	*Pn* (kN) *Alt* 1	*Pn* (kN) *Alt* 2	*Pn* (kN) *Alt* 3	*Pn* (kN) *Alt* 4	*Put* (kN)	$\frac{Alt\ 1}{Put}$	$\frac{Alt\ 2}{Put}$	$\frac{Alt\ 3}{Put}$	$\frac{Alt\ 4}{Put}$
500	355	225.26	225.26	225.26	225.26	224.18	1.0048	1.0048	1.0048	1.0048
650	355	217.67	217.67	218.87	218.87	208.86	1.0422	1.0422	1.0479	1.0479
800	355	202.00	202.00	211.11	211.11	195.56	1.0329	1.0329	1.0795	1.0795
950	355	186.21	186.21	202.16	202.16	190.58	0.9771	0.9771	1.0608	1.0608
1100	355	173.44	173.44	192.13	192.13	172.30	1.0066	1.0066	1.1151	1.1151
1250	355	163.58	163.58	181.35	181.35	170.61	0.9588	0.9588	1.0630	1.0630

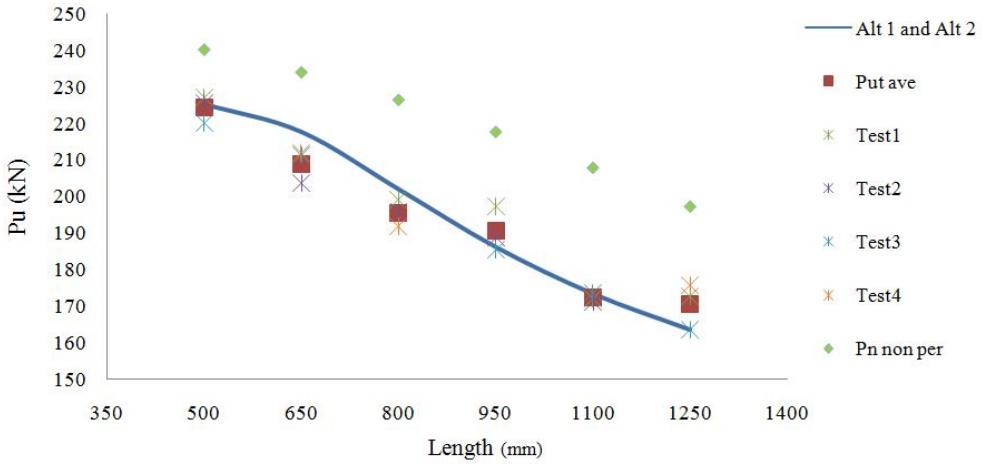

Fig. 15 Relationship between *Pu* and the column length which illustrates the accuracy of Alternative 1 and Alternative 2

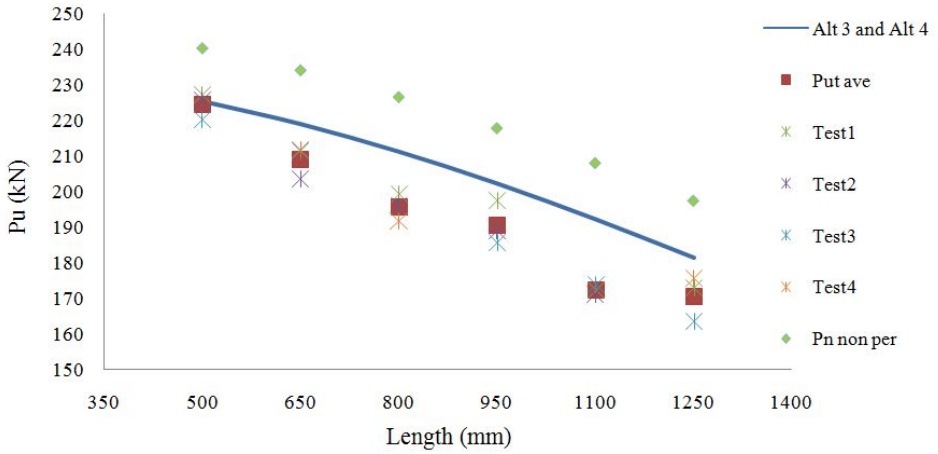

Fig. 16 Relationship between *Pu* and the column length which illustrates the accuracy of Alternative 3 and Alternative 4

Graphs in Figs. 15-16 shows how imprecise is the old method for calculating the column nominal strength, by using the Direct Strength method, without taking into consideration the effect of the perforations of the column. It is clear from the graphs how inaccurate are the determined results (the error discrepancies between 7 to 21%), compared to the results obtained from the experimental tests. However, for the new alternatives, the results show a good accuracy compared to the experimental results. When the graph in Fig. 15 is compared to the graph in Fig. 16, it was clear that Alternative 1 and Alternative 2 give more accurate results (the error discrepancies between 0.5 to 4%) than Alternative 3 and Alternative 4 (the error discrepancies between 0.5 to 11%).

5. Conclusions

The main conclusions of the experimental study that was applied on columns of the same cross-section but of different lengths, can be summarized as follows:

- One of the best ways to determine the effective center of gravity of a steel storage rack column is carrying out experimental tests, by changing the location of the load application point along the symmetry plane of the cross-section and investigating the position that gives the maximum failure load, i.e., the position of the effective center of gravity.
- Buckling occurs at the web of the cross-section, when the load application point is away from the effective center of gravity towards the web.
- Buckling occurs at the flanges of the cross-section, when the load application point is away from the effective center of gravity towards the flanges.
- The load-displacement curves of the tested specimens to determine the effective center of gravity are bounded between two curves. The first curve is the one obtained for the case where the load is applied at the effective center of gravity, at which we get the maximum ultimate load, and it is the upper bound curve. The second curve is the one obtained for the case where the load is applied at the furthest load application point from the effective center of gravity, at which we get the lowest ultimate load, and it is the lower bound curve. (see Fig. 6).
- As the column length increases, the stiffness and the ultimate failure load decrease. (see Fig. 12).
- The displacement levels corresponding to the ultimate failure load are close. (see Fig. 12).
- Local buckling mode, although might have occurred, was not visually detected even in the stub column tests.
- It is observed that the distortional buckling was the dominating buckling mode for all of the tests. For columns of length 1250 mm and 1100 mm, small effects of flexural buckling was noticed.

The main conclusions of the analytical study can be summarized as follows:

- The conventional method for calculating the column nominal strength, using the Direct Strength Method without taking into consideration the effect of perforations along the length of the member, gave imprecise results, (the error discrepancies between 7 to 21%) compared to the experimental test results (see Table 6).
- The different alternatives of the recently proposed approach show a good accuracy compared to the experimental results. Alternative 1 and Alternative 2 gave more accurate

results (the error discrepancies between 0.5 to 4%) than Alternative 3 and Alternative 4 (the error discrepancies between 0.5 to 11.5%) (see Table 7).

Generally, results obtained from the experimental and analytical studies compare very well. This indicates the validity of the recently proposed approach for predicting the ultimate strength of steel storage rack columns with perforations along their length.

References

AISI (2004), Appendix 1: Design of Cold-Formed Steel Structural Members Using the Direct Strength Method; American Iron and Steel Institute, Washington, D.C., USA.

ANSI MH16.1 (2010), Specification for the Design,Testing and Utilization of Industrial Steel Storage Racks; Rack Manufacturers Institute, NC, USA.

Casafont, M., Pastor, M.M., Roure, F. and Peköz, T. (2011), "An experimental investigation of distortional buckling of steel storage rack columns", *Thin-Wall. Struct.*, **49**(8), 933-946.

Casafont, M., Pastor, M., Roure, F., Bonada, J. and Peköz, T. (2013), "Design of steel storage rack columns via the direct strength method", *J. Struct. Eng.*, **139**(5), 669-679.

EN15512 (2009), Steel static stroage systems: Adjustable pallet racking systems; European Standard, European Committee for Standardization, Brussels, Belgium.

Freitas, A.M.S., Freitas, M.S.R. and Souza, F.T. (2005), "Analysis of steel storage rack columns", *J. Construct. Steel Res.*, **61**(8), 1135-1146.

Kwon, Y.B. and Park, H.S. (2011), "Compression tests of longitudinally stiffened plates undergoing distortional buckling", *J. Construct. Steel Res.*, **67**(8), 1212-1224.

LERMA (2013), Distortional buckling strength of American type cold formed rack columns; Laboratori d'elasticitati Resisténcia de Materials, May.

Li, Z. and Schafer, B.W. (2010), Buckling analysis of cold-formed steel members with general boundary conditions using CUFSM: conventional and constrained finite strip methods. www.ce.jhu.edu/bschafer/cufsm/

Pastor, M.M., Casafont, M. and Roure, F. (2009), "Optimization of cold-formed steel pallet racking cross-sections for flexural-torsional buckling with constraints on the geometry", *Eng. Struct.*, **31**(11), 2711-2722.

Peköz, T., Casafont, M., Roure, F., Somalo, M.R., Kıymaz, G., Pastor, M.M. and Bonada, J. (2013), "Current research on cold-formed steel industrial racks", *Proceedings of the 5th Steel Structures Symposium*, Istanbul, Turkey, November.

Roure, F., Pastor, M.M., Casafont, M. and Somalo, M.R. (2011), "Stub column tests for racking design: Experimental testing, FE analysis and EC3", *Thin-Wall. Struct.*, **49**(1), 167-184.

Sarawit, A. (2006), CUTWP Thin-walled section properties, www.ce.jhu.edu/bschafer/cutwp/

Schafer, B.W. (1997), "Cold-formed steel behavior and design: Analytical and numerical modeling of elements and members with longitudinal stiffeners", Ph.D. Dissertation; Cornell University, Ithaca, NY, USA.

Schafer, B.W. (2006a), *Direct Strength Method* (*DSM*) *Design Guide*, American Iron and Steel Institute; Washington, D.C., USA.

Schafer, B.W. (2006b), "Review: The Direct Strength Method of Cold-Formed Steel Member Design", In: *Stability and Ductility of Steel Structures*, Lisbon, Portugal, September.

Schafer, B.W. (2008), "Review: The Direct Strength Method of cold-formed steel member design", *J. Construct. Steel Res.*, **64**(7-8), 766-778.

Schafer, B.W. (2011), "Cold-formed steel structures around the world: A review of recent advances in applications, analysis and design", *Steel Construct.*, **4**(3), 141-149.

Von Karman, T., Sechler, E.E. and Donnell, L.H. (1932), "The strength of thin plates in compression",

Transactions ASME, **54**(4), 53-57.
Yu, W.W. and LaBoube, R.A. (2010), *Cold-Formed Steel Design*, (4th Edition), John Wiley & Sons, Inc., Hoboken, NJ, USA.

CC